Optics Letters

UV-enhanced photorefractive response rate in a thin-film lithium niobate microdisk

Jiankun Hou,[1] Boyi Xue,[1] Ruixin Ma,[1] Simin Yu,[2] Yicheng Zhu,[1] Xianfeng Chen,[3] Juanjuan Lu,[2,4] and Wenjie Wan[1,3,*]

[1]University of Michigan-Shanghai Jiao Tong University Joint Institute, Shanghai Jiao Tong University, Shanghai 200240, China
[2]School of Information Science and Technology, Shanghai Tech University, Shanghai 201210, China
[3]School of Physics and Astronomy, Shanghai Jiao Tong University, Shanghai 200240, China
[4]lujj2@shanghaitech.edu.cn
*wenjie.wan@sjtu.edu.cn

Received 18 April 2024; revised 25 May 2024; accepted 26 May 2024; posted 28 May 2024; published 12 June 2024

The photorefractive (PR) effect plays a critical role in emerging photonic technologies, including dynamic volume holography and on-chip all-optical functionalities. Nevertheless, its slow response rate has posed a significant obstacle to its practical application. Here, we experimentally demonstrate the enhancement of the PR response rate in a high-Q thin-film lithium niobate (TFLN) microdisk under UV light irradiation. At an irradiation intensity of 30 mW/cm^2, the PR effect achieves a high response bandwidth of approximately 256 kHz. By employing this UV-assisted PR effect, we have achieved rapid laser-cavity locking and self-stabilization, where perturbations are automatically compensated. This technique paves the way toward real-time dynamic holography, editable photonic devices on a lithium niobate platform, and high-speed all-optical information processing.

https://doi.org/10.1364/OL.527579

Since the first discovery by Ashkin in 1966 [1], the photorefractive (PR) effect in lithium niobate (LN) has garnered significant attention and has been extensively researched [2]. The PR effect arises from the interaction between the photo-excited space-charge field and the subsequent electro-optic effect, leading to a modulation of the refractive index in the medium [3]. Remarkably, this effect can be effectively erased through optical irradiation or high-temperature treatment, making it a highly promising candidate for refractive index engineering in LN [4]. Combined with the excellent optical properties of LN, the PR effect presents a potential avenue for precise control over the structural characteristics of micro-nano integrated optics. Over the past few years, the PR effect in LN has played a pivotal role in optical field modulation and optical information processing; e.g., it has enabled many novel optical applications like non-volatile storage [5], multi-spectral manipulation [6], phase-conjugate mirrors [7], and dynamic holographic 3D displays [8,9]. Additionally, on the LN-integrated photonic platform, the PR effect has facilitated the implementation of spatial optical solitons [10], all-optical switches [11], and sub-wavelength gratings [12]. Although numerous optical functionalities based on the PR effect in LN have been developed in recent years, the wide bandgap of LN limits the efficiency of the PR effect, resulting in slow response (in the order of minutes), low modulation intensities, and poor sensitivity, all of which represent challenges hindering the further application of the PR effect in LN.

Previous experimental investigations have shown that the bandgap width of LN is nearly around the photon energy of UV light [13]. Consequently, when irradiated with UV light, it is capable of exciting ions located in deep energy levels or even within the valence band. This excitation process results in an increased concentration of conduction band electrons within the LN crystal, thereby enhancing the PR effect [14]. The response rate of the PR effect in LN crystals is primarily limited by the speed of electron diffusion [15,16], which is very slow. To circumvent this limitation to obtain a shorter response time or a faster response rate, ion doping has been introduced in bulk crystals, resulting in a notable reduction of the response time to 13 ms in bismuth-magnesium co-doped LN [17]. Furthermore, the optical field can be significantly enhanced in high-Q thin-film lithium niobate (TFLN) whispering gallery mode (WGM) microcavities [18,19], favoring the realization of the PR effect [20], and the PR effect can exhibit a very short response time of 20.85 ms [21]. Additionally, the phenomenon of optical mode splitting induced by the PR effect in microcavities has also been observed [22,23], which holds potential for applications in all-optical programmable devices. Nevertheless, the current response rate of the PR effect still falls short of meeting the stringent demands of high-speed information processing, necessitating further research and innovation to overcome this challenge.

In this Letter, we propose and demonstrate a technique to enhance the PR response rate by illuminating UV light on the TFLN microdisk. When a LN crystal is irradiated with 254 nm UV light, electrons in the valence band are excited to the conduction band, resulting in an increase in the free electron density and a reduction in the buildup and decay time τ_{sc} of the spatial charge field E_{sc}. We demonstrate that when a TFLN microcavity is uniformly irradiated with UV light, the overall wavelength shift of the resonant mode is suppressed, the forward (from shorter to longer wavelengths) wavelength scanning spectrum

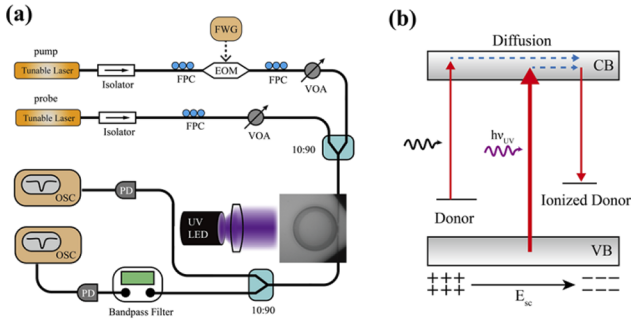

Fig. 1. Experimental setup and PR effect mechanism concept diagram. (a) Schematic illustration of the experimental setup for the UV-enhanced PR response rate. The UV beam is uniformly irradiated on the microdisk after passing through a lens. EOM, electro-optic modulator, VOA, variable optical attenuator; FPC, fiber polarization controller; PD, photodetectors; OSC, oscilloscope; FWG, functional wave generator. (b) Energy-level diagram of LN under UV irradiation illustrating the processes of the PR effect. CB, conduction band; VB, valence band.

of the resonant mode is compressed, and the backward (from longer to shorter wavelengths) wavelength scanning spectrum is broadened. In particular, the PR response rate increases with UV irradiation intensity, reaching 256 kHz under 30 mW/cm^2 exposure. Finally, we have achieved UV-assisted PR fast stable laser-cavity locking, which exhibits high immunity to interference and stability. These results not only hold great promise for all-optical control in lithium niobate-on-insulator (LNOI) integrated photonics but also provide a novel approach for enhancing PR response rates in optical information storage and volume holography.

Figure 1(a) illustrates the schematic of the experimental setup, where a UV (254 nm) beam is uniformly irradiated onto the microcavity after passing through a convex lens. The pump and probe beams are combined into a tapered fiber through a 10:90 fiber beam splitter and then excite the modes in the microdisk resonator through evanescent field coupling. The pump (CTL, Toptica Photonics) and probe (New Focus, TLB-6728) have different wavelengths, and their polarization and power are controlled by FPC and VOA, respectively. The device utilized in our experiment is a high-Q (~10^5) LN microdisk resonator, crafted on a Z-cut commercial LNOI wafer (shown in the inset of Fig. 1(a)). This resonator, with a thickness of 600 nm and a diameter of 80 μm, rests upon a 2-μm-tall silica pedestal. The device was patterned through UV photolithography and chemo-mechanical polishing (CMP) with a wedge angle of 10° [24]. Hence, the coupling efficiency can be controlled by adjusting the position of the contact point at the edge of the microdisk [25].

Firstly, we investigate the mechanism of the UV light's impact on the PR effect in LN crystals, as depicted in Fig. 1(b). The PR effect in LN crystals involves several fundamental physical processes: photoionization, diffusion, and capture leading to the formation of a space-charge field E_{sc} and subsequent changes in refractive index resulting from the electro-optic effect. With LN's 3.8 eV bandgap [26], UV irradiation prompts valence electrons to transition to the conduction band, raising its electron concentration. In the long-period grating approximation, the PR response time equals to the dielectric relaxation time, so the expression for the generation and decay time τ_{sc} of the space-charge field E_{sc} is as follows [3,15]:

$$\tau_{sc} = \frac{\varepsilon\varepsilon_0}{e\mu_e n_c}, \quad \alpha_{sc} = \frac{1}{\tau_{sc}}, \tag{1}$$

where $\varepsilon\varepsilon_0$ is the permittivity of the crystal, n_c denotes the total density of charge carriers, e is the electronic charge, μ_e is the electronic mobility, and α_{sc} represents the relaxation rate of the space-charge field. It is evident that an increase in n_c will lead to a decrease in τ_{sc}, indicating that UV light irradiation can enhance the response rate of the PR effect. In this study, we controlled the power of the pump to produce only the PR effect, insufficient to induce the thermo-optical effect. Under such conditions, the cavity dynamics are primarily influenced by the PR effect and can be described by the following equation [27]:

$$\frac{da}{dt} = \left(i\Delta - \frac{\gamma}{2}\right) a - ig_E E_{sc} a + \sqrt{\gamma_{ex}} a_{in}, \tag{2}$$

$$\frac{dE_{sc}}{dt} = -\alpha_{sc} E_{sc} + \eta_{sc} |a|^2. \tag{3}$$

Here a and a_{in} represent the amplitudes of the intracavity field and the input field, respectively. The pump detuning, denoted as Δ, is the difference between the resonant frequency ω_0 and the pump frequency ω_p. γ, and γ_{ex} refer to the total decay rate and external decay rate of the mode, respectively. The term $g_E E_{sc}$ represents the resonance frequency shift resulting from the PR effect, where E_{sc} is the average space-charge-induced electric field and $g_E = n_0^2 \omega_0 r_{33}/2$ is the electro-optic coupling coefficient contributed by the Pockels effect [26]. When the pump is coupled to the microdisk and excites the resonant mode, the space-charge field is generated through optical absorption-induced ionization and subsequent charge distribution [3], expressed as Eq. (3), where η_{sc} denotes the generation coefficient, which is assumed independent of the optical power for simplicity. Equations (1)–(3) describe the intracavity dynamics within the optical cavity during UV irradiation [27,28]. Evidently, UV irradiation increases α_{sc}, resulting in changes in the transmission spectrum. The PR effect response faster than the laser scan rate causes transmission spectrum deformation. A slower response lags behind intracavity changes, resulting in a temporally uniform field [12], leading to an overall blueshift of the resonant mode without any waveform distortion. In the next section, we conducted a series of experiments to investigate the specific impact of UV irradiation on the PR effect.

To investigate the PR effect both with and without UV irradiation, we choose a fundamental transverse-electric (TE) mode operating at 1549.48 nm. In our experiments, we apply laser scans that traverse the resonance in both forward and backward directions at different input powers and scan rates, as illustrated in Fig. 2. The input power is regulated by a VOA, while the scan rate is adjusted through the periodically modulated triangular wave. For the scans presented in both Figs. 2(a) and 2(c), the scan rate is maintained at 1 nm/s. Without UV radiation, as shown in Fig. 2(a), the time taken by the laser to scan through the resonant modes is approximately 0.022 s, which is significantly shorter than the response time of the PR effect (~100 s). Therefore, the PR effect perceives the time-periodic pulse-modulated intracavity intensity as an average intensity, which is proportional to the input power [12]. As a result, the final transmission spectrum exhibits an overall blueshift, while the waveform remains unchanged. However, in the presence of UV radiation, depicted in Fig. 2(c), as the input power rises from

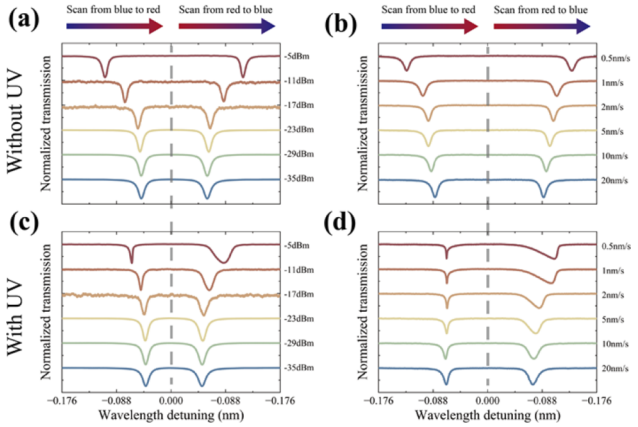

Fig. 2. Experimentally measured transmission spectra of the TFLN microdisk. (a) Forward and backward laser-scanned transmission spectra of the microdisk under different optical powers with a fixed scan rate 1 nm/s without UV irradiation. The power in the tapered fiber varies from −5 to −35 dBm. (b) Forward and backward transmission spectra of the same microdisk resonator with different scan rates at a fixed input power of −5 dBm without UV irradiation. The scan rate varies from 0.5 to 20 nm/s. (c) and (d) display the results of the transmission spectra with UV irradiation under the same conditions as (a) and (b), respectively. The transmission spectra are normalized with respect to the reference power meter.

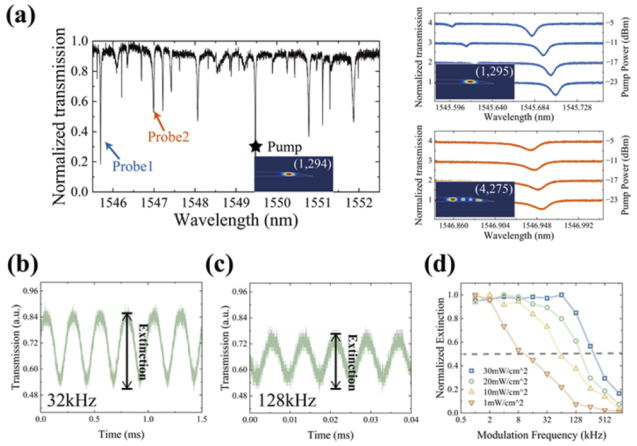

Fig. 3. Impact of UV irradiation power on the PR response rate. (a) Normalized transmission spectrum of the TFLN microdisk at telecommunication wavelengths. The mode where probe1 is excited and the mode where the pump is excited to possess the same radial mode number, and the FSR is 3.78 nm. The right part shows the detuning of probe1 (blue) and probe2 (orange) at different pump powers. Inset: electric field patterns. (b) and (c) Temporal response (probe1) of the dynamic control with the modulation rate of 32 and 128 kHz, respectively, under UV irradiation at 20 mW/cm^2. (d) shows the normalized extinction of the transmission of probe1 plotted against modulation rates under varying UV irradiation powers. The extinction values are normalized to the maximum value observed, and the dashed line represents the modulation bandwidth.

−35 to −5 dBm, the resonance shape undergoes a notable deformation but the overall blueshift is suppressed. The PR effect leads to a decrease in the refractive index, causing the linewidth of the resonant mode to narrow during forward scanning and broaden during backward scanning. Subsequently, we fix the input power at −5 dBm and vary the laser scan rate from 0.5 to 20 nm/s, as exhibited in Figs. 2(b) and 2(d). In the absence of UV irradiation (Fig. 2(b)), the resonance maintains its Lorentzian shape and exhibits a blueshift as the scan rate decreases during scanning from blue to red. Conversely, with UV irradiation (Fig. 2(d)), the resonance shape transforms from a Lorentzian-like shape to a triangular shape, resembling the characteristics of the thermo-optic effect in the opposite way [29]. Additionally, the small redshift of the resonant mode in the lowest transmission spectra in Figs. 2(c) and 2(d) where the PR effect is very weak, is caused by the temperature increase of the LN microdisk after absorbing UV photons. This observation suggests that the PR effect response rate under UV irradiation could be on par with the thermo-optic effect response, attaining up to the kHz order of magnitude [30]. We expect this effect to also apply to the x-cut TFLN microresonator, as the increase in electron concentration due to UV irradiation is not dependent on the crystal orientation.

To characterize the relationship between UV irradiation and PR response rate, we further investigate the magnitude of PR response rate under different UV irradiation intensities. The refractive index change induced by the PR effect can act on all resonant modes supported by the microdisk resonator, so we can read the PR response rate using another beam of probe light. As shown in Fig. 1(a), the power intensity of the pump light is modulated by an EOM driven by RF signals, and the probe signal at another wavelength is detected by a PD after passing through a bandpass filter to filter out the pump light. By fixing the wavelength of the probe at the red-detuned side of the resonant mode, where the wavelength of the probe is slightly longer than the resonant wavelength, the intensity modulation of the pump light will be observed in the transmission spectrum of the probe through the PR effect. The left part of Fig. 3(a) shows the long-range transmission spectrum of the microdisk from 1545.5 to 1552.5 nm, where probe1 at 1545.7 nm has the same radial mode number as the pump, while probe2 at 1546.95 nm is another family of resonant modes. Due to the high degree of overlap between modes in the same family, the detuning of probe1 is more affected by the pump power than probe2, as shown in the right part of Fig. 3(a). Hence, probe1 is selected to read the PR response rate. The intensity of UV irradiation received by the microdisk can be modulated by altering the distance between the UV LED and the microdisk. Figures 3(b) and 3(c) respectively show the modulated transmission of probe1 in different frequencies of sine waves corresponding to 32 and 128 kHz under UV irradiation at 20 mW/cm^2. When the modulation rate reaches 32 kHz, the transmission of probe1 follows the modulation very well, showing a large modulation extinction of 90%. But when the modulation rate approaches 128 kHz, the modulation extinction decreases obviously, shown as Fig. 3(c). Figure 3(d) depicts the power extinction of the transmission of probe1 against the modulation rate at different UV irradiation intensities. Under 30 mW/cm^2 UV light irradiation, the bandwidth of the PR response can reach approximately 256 kHz, and the corresponding relaxation time is 3.9 μs, which is much faster than the situation without UV irradiation (~60 s) [12].

Finally, we demonstrate a technique to rapidly stabilize the laser-cavity lock utilizing the UV-assisted PR effect. As shown in Fig. 4, we control the laser backward scan across the resonant mode, pause at different transmission points, and observe the evolution of the transmission spectrum over time. It can be seen

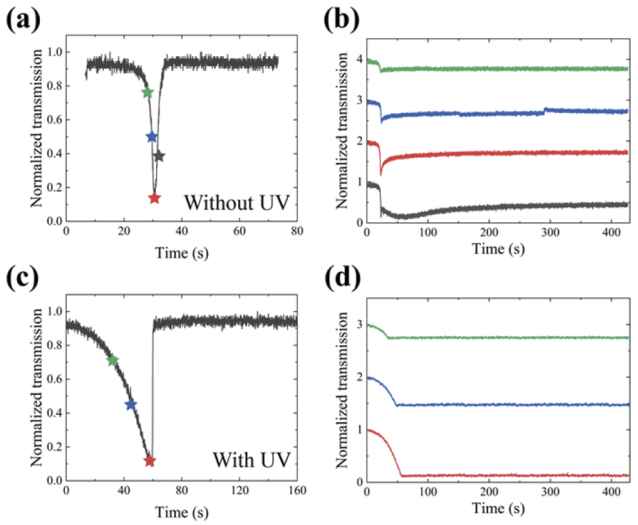

Fig. 4. UV-assisted PR fast locking during the downward wavelength scan. (a) and (c) Backward laser-scanned transmission spectra of the same mode without and with UV irradiation, respectively, and the scan rate is 0.01 nm/s. The wavelength scanning of the laser is paused at different moments (marked with different color stars), and corresponding transmission spectra versus time are shown in (b) and (d). Without UV irradiation, the transmission spectra require approximately 100 s to stabilize. However, with UV irradiation, the transmission spectra stabilize instantly, and the noise is much lower than when there is no UV irradiation, demonstrating that perturbations are self-compensated.

that without UV irradiation, the response time of the PR effect is very long, the system needs about 100 s to stabilize, and the noise is relatively large, as shown in Figs. 4(a) and 4(b). In this case, it is difficult to accurately lock the laser at the resonant frequency ($\Delta = 0$) [28]. However, upon exposure to UV irradiation of 20 mW/cm^2, the resonance shape transforms into a triangular shape as depicted in Fig. 4(c). Remarkably, once the laser wavelength scanning ceases, the system promptly attains a stable equilibrium state and sustains it over an extended period, as illustrated in Fig. 4(d). In fact, the physical principle corresponding to this phenomenon is the same as thermo-optic locking, except that the refractive index here decreases instead of increases. Therefore, this is also a self-stable equilibrium, in which disturbances can compensate themselves, as evidenced by the good signal-to-noise ratio in Fig. 4(d). Using this technique, we can accurately lock the laser at the resonant frequency for a long time ($\Delta = 0$), as indicated by the red star in Fig. 4(c).

In conclusion, we have demonstrated that the response rate of the PR effect can be significantly enhanced by UV irradiation in a TFLN microdisk. We observe that the stronger the UV irradiation intensity, the faster the response rate of the PR effect. Under 30 mW/cm^2 UV irradiation, we achieve a modulation bandwidth of approximately 256 kHz for the PR effect, which has never been realized in LN crystals and resonators [17,21,31–34]. Furthermore, we demonstrate a rapidly stabilizing laser-cavity locking technique utilizing the UV-assisted PR effect, enabling the laser to be locked at the resonant frequency for extended periods, achieving self-stabilization. This opens up new avenues for refractive index modulation in all-optical signal processing and nonlinear integrated photonics applications [35,36]. Additionally, it provides a new approach for increasing the response rate in real-time dynamic holographic 3D displays and high-speed signal processing based on PR materials.

Funding. The National Key Research and Development Program of China (2023YFA1407200, 2023YFB3906400); the National Science Foundation of China (12274295, 92050113).

Disclosures. The authors declare no conflicts of interest.

Data availability. Data underlying the results presented in this paper are not publicly available at this time but may be obtained from the authors upon reasonable request.

REFERENCES

1. A. Ashkin, G. D. Boyd, J. M. Dziedzic, *et al.*, Appl. Phys. Lett. **9**, 72 (1966).
2. M. Bazzan and M. Fontana, Appl. Phys. Rev. **2**, 040501 (2015).
3. P. Günter and J.-P. Huignard, eds., *Photorefractive Materials and Their Applications* (Springer, 2006).
4. Y. Kong, F. Bo, W. Wang, *et al.*, Adv. Mater. **32**, 1806452 (2020).
5. K. Buse, A. Adibi, and D. Psaltis, Nature **393**, 665 (1998).
6. H. C. Hsu and P. Han, J. Opt. Soc. Am. A **37**, 219 (2020).
7. C. Mailhan, N. Fressengeas, M. Goetz, *et al.*, Phys. Rev. A **67**, 023817 (2003).
8. Y. Pan, J. Liu, X. Li, *et al.*, IEEE Trans. Ind. Inf. **12**, 1599 (2016).
9. P.-A. Blanche, A. Bablumian, R. Voorakaranam, *et al.*, Nature **468**, 80 (2010).
10. M. Yu, Y. Okawachi, R. Cheng, *et al.*, Light: Sci. Appl. **9**, 9 (2020).
11. M. Li, M. Zhang, and D. Dai, in *Advanced Fiber Laser Conference (AFL2023)*, Vol. 13104 (SPIE, 2024), pp. 1820–1823.
12. J. Hou, J. Zhu, R. Ma, *et al.*, "Subwavelength photorefractive grating in a thin-film lithium niobate microcavity," Laser Photonics Rev. (to be published).
13. A. Dhar and A. Mansingh, J. Appl. Phys. **68**, 5804 (1990).
14. J. Xu, G. Zhang, F. Li, *et al.*, Opt. Lett. **25**, 129 (2000).
15. P. M. Johansen, J. Opt. A: Pure Appl. Opt. **5**, S398 (2003).
16. Y. Kong, F. Liu, T. Tian, *et al.*, Opt. Lett. **34**, 3896 (2009).
17. S. Wang, Y. Shan, D. Zheng, *et al.*, Opto-Electron. Adv. **5**, 210135 (2022).
18. R.-R. Xie, G.-Q. Li, F. Chen, *et al.*, Adv. Opt. Mater. **9**, 2100539 (2021).
19. M. Zhang, C. Wang, R. Cheng, *et al.*, Optica **4**, 1536 (2017).
20. A. A. Savchenkov, A. B. Matsko, D. Strekalov, *et al.*, Phys. Rev. B **74**, 245119 (2006).
21. H. Jiang, R. Luo, H. Liang, *et al.*, Opt. Lett. **42**, 3267 (2017).
22. J. Liu, T. Stace, J. Dai, *et al.*, Phys. Rev. Lett. **127**, 033902 (2021).
23. Y. Xu, A. A. Sayem, C.-L. Zou, *et al.*, Opt. Lett. **46**, 432 (2021).
24. J. Hou, J. Lin, J. Zhu, *et al.*, PhotoniX **3**, 22 (2022).
25. J. Hou, J. Zhu, R. Ma, *et al.*, "Enhanced frequency conversion in parity-time symmetry line," arXiv, arXiv:2402.06200 (2024).
26. C. Thierfelder, S. Sanna, A. Schindlmayr, *et al.*, Phys. Status Solidi (c) **7**, 362 (2010).
27. Y. Xu, M. Shen, J. Lu, *et al.*, Opt. Express **29**, 5497 (2021).
28. X. Sun, H. Liang, R. Luo, *et al.*, Opt. Express **25**, 13504 (2017).
29. T. Carmon, L. Yang, and K. J. Vahala, Opt. Express **12**, 4742 (2004).
30. X.-X. Hu, J.-Q. Wang, Y.-H. Yang, *et al.*, Opt. Express **28**, 11144 (2020).
31. M. Leidinger, C. S. Werner, W. Yoshiki, *et al.*, Opt. Lett. **41**, 5474 (2016).
32. Y. Kong, S. Liu, and J. Xu, Materials **5**, 1954 (2012).
33. M. Kösters, B. Sturman, P. Werheit, *et al.*, Nat. Photonics **3**, 510 (2009).
34. D. Zheng, Y. Kong, S. Liu, *et al.*, Sci. Rep. **6**, 20308 (2016).
35. J. Yang, L. Yuan, T. Qin, *et al.*, Optica **8**, 1448 (2021).
36. Y. Chen, F. Zhang, T. Qin, *et al.*, Optica **9**, 971 (2022).